Microluminescence from $Cd_{1-x}Mn_xTe$ magnetic quantum dots containing only a few Mn ions

P. Wojnar,[1] J. Suffczyński,[2] K. Kowalik,[2] A. Golnik,[2] G. Karczewski,[1] and J. Kossut[3]
[1]*Institute of Physics, Polish Academy of Sciences, Al. Lotnikow 32/46, 02-668 Warsaw, Poland*
[2]*Institute of Experimental Physics, Warsaw University, Hoża 69, 00-681 Warsaw, Poland*
[3]*Institute of Physics, Polish Academy of Sciences, and ERATO Semiconductors Spintronics Project, Al. Lotnikow 32/46, 02-668 Warsaw, Poland*

(Received 3 August 2006; revised manuscript received 30 November 2006; published 2 April 2007)

Self-assembled magnetic $Cd_xMn_{1-x}Te$ quantum dots (QDs) embedded in nonmagnetic $Zn_{0.6}Cd_{0.4}Te$ were grown by molecular beam epitaxy. We achieved a large degree of dilution of Mn ions inside the QDs, $x_{Mn}=0.003$, which allowed us to study single QDs containing only few Mn ions. The insight into properties of these structures was obtained by performing measurements of photoluminescence in an external magnetic field with a high spatial resolution by using immersion reflection objective. Approximate number of Mn ions inside dots and the size of the dots were found by comparison of the magnetic field evolution of the corresponding photoluminescence lines with calculations in terms of a muffin tin model developed originally to describe bound magnetic polarons.

DOI: 10.1103/PhysRevB.75.155301 PACS number(s): 78.67.Hc, 75.50.Pp, 75.75.+a, 78.55.−m

I. INTRODUCTION

In the family of II-VI diluted magnetic semiconductors (DMS), the presence of paramagnetic Mn ions in the crystal lattice results in a strong enhancement of their spin-related properties such as the Zeeman splitting, the Faraday rotation, etc. This is due to a strong *sp-d* coupling between band carriers and localized Mn magnetic moments. This coupling can be used to manipulate very effectively the spins of the carriers by means of an even modest external magnetic field. Extremely interesting, from the point of view of applications in spintronic devices, are zero-dimensional objects composed of DMS, in particular, self-assembled II-VI quantum dots. Their magnetic properties are determined by several parameters, like the number of Mn ions inside the QD, their position in the dot and the size of the dot itself. The knowledge of all these parameters is necessary in order to manipulate the spin of carriers confined in the QDs in a controlled manner.

The diluted magnetic QDs have already been grown using various material systems basing on II-VI semiconductors: CdMnTe/ZnTe,[1–7] CdSe/ZnMnSe,[8–11] CdMnTe/CdMgTe,[12] and CdMnSe/ZnSe.[13,14] The properties of these structures strongly depend on the method of introducing Mn ions into the structure and the material system that is used. Directly related to the choice of the materials is the position of the energy of the excitonic emission from the QDs ensemble with respect to the intense internal Mn optical transition occurring at the energy of about 2.0 eV. In the case when the excitonic emission is above the latter energy, a very strong effective transfer of the excitation to the Mn subsystem occurs which considerably decreases the quantum efficiency of the photoluminescence from the quantum dots[10,11,13] and results in a significant shortening of the excitonic lifetime.[10] In order to avoid these effects we choose carefully the composition of the barrier for the $Cd_{1-x}Mn_xTe$ magnetic QDs. Using $Zn_{0.6}Cd_{0.4}Te$ instead of pure ZnTe barriers we decrease effectively the barrier potential and, as an effect, the QD emission band is redshifted well below the energy of the internal Mn transition.

When the excitonic emission is below the intra-Mn transition, we must take into account the presence of effects connected with magnetic polaron (MP) formation,[8–10,12] i.e., spontaneously formed ferromagnetic domains within a diluted magnetic QD. They also form as result of the strong exchange interaction between the magnetic moment of the Mn ions and the spin of the carriers decreasing the total energy of the system of the Mn and the charge carriers. In the case of $Cd_{1-x}Mn_xTe$ in the bulk form, magnetic polarons bound to either donors or acceptors are stable. Due to the spatial confinement of the carriers by the QD potential, however, one can expect the polaronic effect to be particularly strong in the zero-dimensional environment even when the impurities are absent. On the other hand, polaronic effects are not important in the case when the exciton energy exceeds 2.0 eV, the energy of the internal Mn transition, because the lifetime of excitons decreases so much that it becomes shorter than the formation time of the MP.[10]

Several different attempts were made in order to introduce Mn ions into nonmagnetic QDs. Most of them used the interdiffusion of Mn from the diluted magnetic barrier[8–11] or from a remote Mn-rich layer.[1,3] Some other studies made use of formation of so-called "natural QDs" formed by the potential fluctuations of a thin diluted magnetic quantum wells.[12]

In our QDs, the Mn ions are introduced directly into the QDs themselves, intentionally into the central layer of the QD. Moreover, we monitor the QD formation process by a distinct two-dimensional to three-dimensional (2D-3D) growth mode transition in the RHEED pattern after applying the method described in Ref. 15. As already mentioned, the PL of our QDs ensemble lies below the energy of the internal Mn transition, i.e., in the regime where the magnetic polaron formation is expected. Similar to the case of Refs. 1–4 and Refs. 8 and 9, we use high spatial resolution photoluminescence (μ-PL) measurements in an external magnetic field in order to study magneto-optical properties of individual diluted magnetic QDs. The approximate number of Mn ions inside of the dots is determined by a comparison of the experimental data with theoretical calculations in terms of the muffin tin model, which is known to describe properly the main features of the system whose optical properties are de-

termined by formation of magnetic polarons.[16–18]

II. SAMPLES

The samples are grown in a standard molecular beam epitaxy apparatus. On a semi-insulating GaAs (001) substrate, a 4 μm thick CdTe buffer is first deposited. It is followed by 1 μm $Zn_{0.6}Cd_{0.4}Te$ barrier layer. The quantum dot layer is formed from five monolayers of a large lattice constant material of which the two lower and the two uppermost monolayers are made of pure CdTe, whereas the Mn ions are added only into the central CdTe monolayer. This QD layer is deposited in atomic layer epitaxy mode, i.e., by alternated opening of the cation and the anion effusion cells. For the $Cd_{1-x}Mn_xTe$ layer deposition, we open Cd and Mn effusion cell simultaneously. The Mn amount of about 0.3% in the CdTe layers we determine from photoluminescence measurements which will be discussed later. The self assembled quantum dots are formed by using the method developed recently by Tinjod *et al.*,[19,15] i.e., we cover the strained CdTe/CdMnTe layers with an amorphous tellurium at low substrate temperature. After thermal desorption of this layer we observe clearly QDs formation by spontaneous 2D-3D growth mode transition in the RHEED pattern. The quantum dots are capped with 100 nm $Zn_{0.6}Cd_{0.4}Te$.

High resolution transmission electron microscopy of our dots (the details of this study to be described elsewhere) reveals that the dots have lens-like shape with the typical in-plane radius of the order of 10 nm and the height of about 2 nm. Knowing the lattice constant and atomic structure of CdTe, we estimate the number of cation sites in such typical QD, N_{cat}=4400. This implies that in the case of Mn amount of 0.3% and under assumption that all the Mn-ions find themselves in the dots, one can expect on the average about 15 Mn ions in such a dot.

III. RESULTS

We perform both standard and spatially resolved PL measurements in an external magnetic field ranging from −6 T to 6 T in the Faraday configuration with the field along the growth axis detecting only one circular polarization [Fig. 1(a)]. By reversing the direction of the magnetic field we change the detected circular polarization. The excitation power is kept as low as possible (35 mW/cm^2) in order to avoid heating effects. For the nonresonant excitation we use frequency doubled YAG laser (532 nm). The signal is dispersed in a 0.6 m monochromator equipped with a 1200 mm^{-1} grating and detected by a charge coupled device camera.

A typical PL spectrum of our QDs consists of a very broad band extending from 1.72 eV to 1.95 eV. Its spectral width is determined by inhomogeneity of the sizes and chemical compositions of the quantum dots in the ensemble. When we increase the magnetic field, the intensity of the whole PL band increases in one circular polarization (σ^+), whereas it decreases in the other polarization (σ^-). In Fig. 1(b), we plot the degree of the circular polarization $\rho=(I_{\sigma+}-I_{\sigma-})/(I_{\sigma+}+I_{\sigma-})$ as a function of the magnetic field, where

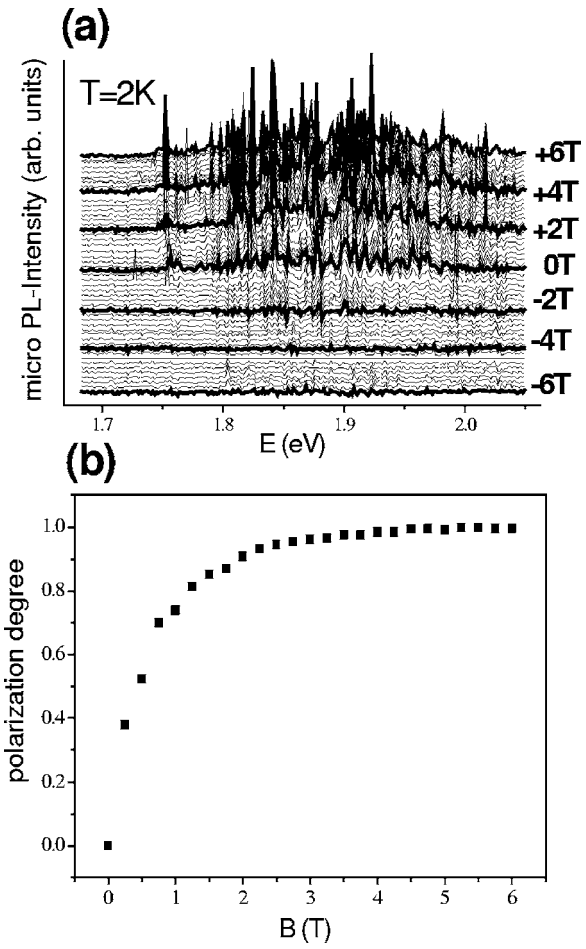

FIG. 1. (a) Microphotoluminescence spectra of $CdMnTe/Zn_{0.6}Cd_{0.4}Te$ QDs with small amount of Mn taken in magnetic fields ranging from −6 T to 6 T (nonresonant excitation with 364 nm argon line), (b) the degree of polarization of photoluminescence from the whole QDs ensemble as a function of the magnetic field at 2 K.

$I_{\sigma+}$ ($I_{\sigma-}$) is the integrated intensity of the whole PL line in σ^+ (σ^-) polarization. We observe that the spectrum is nearly completely polarized already at B=2 T. This polarization results directly from the giant Zeeman splitting of the excitonic level in the QDs which is a consequence of strong exchange interaction of excitons confined in QDs with the Mn ions. Thus, the polarization of PL provides a direct evidence of the incorporation of Mn ions into the QDs.

In the case of the micro-PL, when the excitation spot is less than 1 μm, we observe that the broad PL band splits into a large number of lines each coming from an individual QD. In this work, we focus on the evolution of the shape and spectral position of these lines in the external magnetic field.

Typical PL lines show a clear redshift of their spectral position with the magnetic field increasing [Figs. 2(a), 3(a), and 4(a)]. This effect is a consequence of the giant Zeeman splitting of excitonic levels in the QDs, which is, again, typical for structures containing diluted magnetic semiconductors. Moreover, we observe a quantitatively different behavior of this energy shift in the dots coming from the low energy part of the spectrum and from the high energy part.

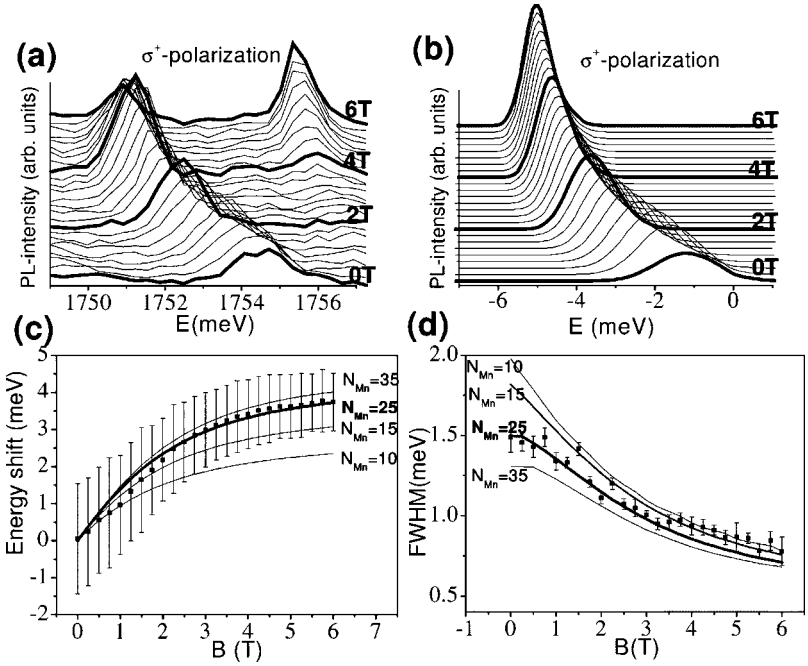

FIG. 2. (a) Magnetic field dependence of an individual diluted magnetic QD from the low energy part of the spectrum (large dot), $T=2$ K. (b) Calculations of the shapes of PL lines in terms of the muffin tin model: $N_{cat}=6600$; $N_{Mn}=25$; $T_{eff}=4.9$ K. (c) Magnetic field dependence of the position of the PL line: experimental points and theoretical calculations in terms of the muffin tin model for QDs with $x=0.0038$, $T=4.9$ K and different sizes (lines). The bold line marks the best fit for $N_{Mn}=25$. The error bars show the spectral widths of the PL lines determined from Gaussian fits. (d) Magnetic field dependence of the spectral width: experiment points and theoretical calculations (lines). The error bars of experimental points show the uncertainties of determination of the spectral width from the Gaussian fit.

The PL lines from the low energy part of the spectrum ($E<1.8$ eV), representing large QDs, show typically relatively large Zeeman shifts 3.5 meV–4.5 meV at 6 T, whereas the dots with the PL line in the high energy part of the spectrum ($E>2.0$ eV) are characterized by smaller energy shifts of 0.7 meV–2 meV at 6 T.

One possible explanation of this effect may be the magnetic polaron formation which, according to several theoretical calculations,[20,16–18] is very sensitive to the size of the QDs, and results in a spontaneous effective intrinsic magnetization. The smaller the quantum QD, the larger the density of the wave function of the carriers interacting with Mn ions and, as effect, the stronger the exchange interaction energy which causes alignment of magnetic moments of Mn ions. Thus, quantum dots with relatively small sizes are characterized by strong intrinsic magnetization which causes their PL lines to be less sensitive to the external magnetic field.

In Fig. 2(a), we present a magnetic field dependence of a typical line from the low energy part of the PL spectrum ($E<1.8$ eV) which represents large quantum dots. Its shape can be well fitted by a Gaussian for all magnetic fields. From these fits we extract the spectral position and the spectral width of the PL line as a function of the magnetic field, which are plotted in Figs. 2(c) and 2(d), respectively.

In Fig. 2(c), we observe that the dependence of the energy shift tends already to saturate at 6 T and its value amounts to 3.8 meV at 6 T. In Fig. 2(d), one observes that a typical spectral width of a PL line from an individual diluted mag-

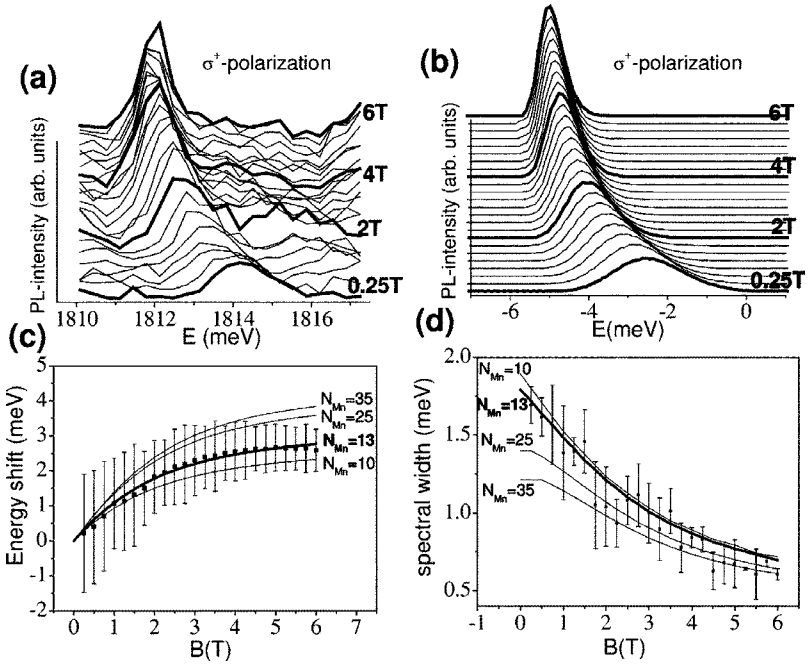

FIG. 3. (a) Magnetic field dependence of an individual diluted magnetic QD from the central part of the spectrum (medium dot), $T=2$ K. (b) Calculations of the shapes of PL lines in terms of the muffin tin model: $N_{cat}=3600$; $N_{Mn}=13$; $T_{eff}=4.9$ K. (c) Magnetic field dependence of the position of the PL line: experimental points and theoretical calculations in terms of the muffin tin model for QDs with $x=0.0036$, $T=4.9$ K and different sizes (lines). The bold line marks the best fit for $N_{Mn}=13$. The error bars show the spectral widths of the PL lines determined from Gaussian fits. (d) Magnetic field dependence of the spectral width: experiment points and theoretical calculations (lines). The error bars of experimental points show the uncertainties of determination of the spectral width from the Gaussian fit.

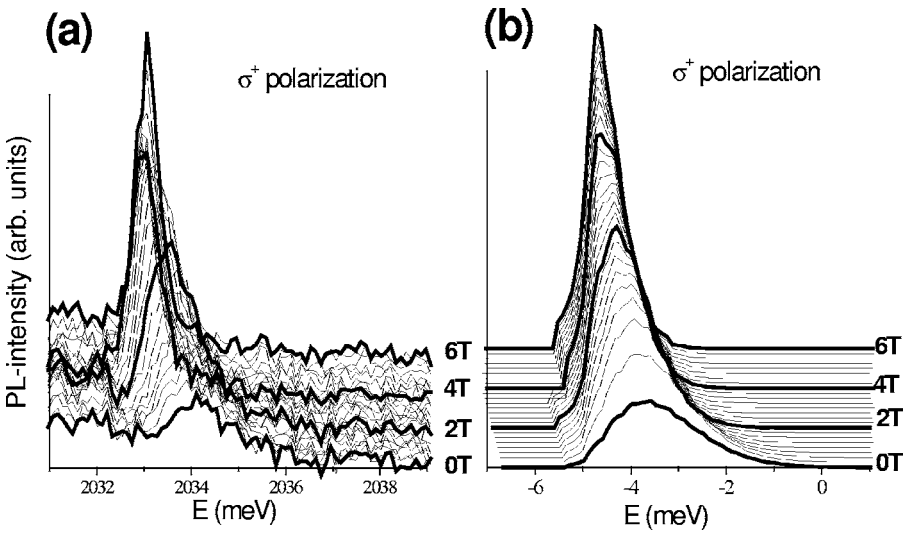

FIG. 4. (a) Magnetic field dependence of an individual diluted magnetic QD from the high energy part of the spectrum (small dot), $T=2$ K. (b) Calculations of the shapes of PL lines in terms of the muffin tin model: $N_{cat}=1500$; $N_{Mn}=5$; $T_{eff}=4.9$ K.

netic QD at 0 T amounts to 1.5 meV which is an order of magnitude larger in comparison with the nonmagnetic CdTe QDs. This finding is consistent with results reported from other diluted magnetic QDs.[4,8,9] With an increasing magnetic field, the spectral width narrows until it reaches the value 0.5 meV at 6 T which is almost a value typical for nonmagnetic QDs.[21,22] The broadening of the PL lines at low magnetic fields is presently understood as due to fluctuations of Mn magnetic moments inside the dot.[4,8,9] By increasing the magnetic field, these fluctuations are suppressed due to alignment of Mn ions along the direction of the magnetic field. At sufficiently strong magnetic field (in our case at 6 T) nearly all Mn ions are aligned.

Individual lines show also a strong σ^+ polarization in the presence of the field. The increase of the intensity in σ+ polarization is directly connected to the giant Zeeman splitting of the excitonic levels in the QDs. At low temperature (2 K in our case), the lower energy branch becomes more densely populated with an increasing magnetic field. At magnetic fields above 2 T, the line is already fully polarized and its integrated intensity does not change anymore. However, the narrowing of the lines causes further increase of the PL intensity at the maximum.

Let us note, that sometimes a second peak appears at about 3 T, as exemplified in Fig. 2(a), which steals the PL intensity from the main peak with increasing magnetic field. This is definitely not a typical feature in magnetic QDs and the most QDs do not show this feature, e.g., PL lines shown in Figs. 3(a) and 4(a). The appearance of this additional peak affects, however, only the intensity of the main PL line, whereas spectral position and spectral width remain as for typical magnetic QDs.

In Figs. 3(a) and 4(a), we present two further PL lines from magnetic QDs coming from the central part of the spectrum ($1.8\ \text{eV} < E < 2.0\ \text{eV}$) and from the high energy part of the spectrum ($E > 2.0$ eV), representing medium sized and small QDs, respectively. They show both qualitatively similar behavior as the PL line from the large dots concerning the energy redshift, a decrease of the spectral width and circular polarization of the spectra. However, the energy shift of the spectral position at 6 T exhibits smaller values, than in the large dots, 2.7 meV in the case of the QD presented in Fig. 3(a) and only 1 meV in the QD from Fig. 4(a).

The spectral position and the spectral width of the PL line from the medium QD, which are extracted from Gaussian fits, are plotted in Figs. 3(c) and 3(d), respectively. In the case of the QD from the high energy part of the spectrum, the line shape exhibits a greater deviation from the regular Gaussian and the subsequent comparison with the model calculations remains at a less quantitative level.

The deviations from the Gaussian shape in the small dots may steam from the fact, that the exciton interacts with only a few Mn ions inside the dot. In this case the magnetization does not exhibit Gaussian fluctuations and is given by a relatively small number of possible Mn ions arrangements.

IV. CALCULATING AN APPROXIMATE NUMBER OF MN IONS IN THE DOTS

In order to find an approximate number of Mn ions coupled to the exciton inside a diluted magnetic QD and the average number of cation sites that the exciton is interacting with, which gives us the information about the size of the dot, we perform an analysis of experimental data which consists of two steps.

In the first step, we use the mean field approximation (MFA) and the virtual crystal approximation (VCA), which, in the case of large dots, results in a Brillouin-like behavior of the PL line position as a function of the external magnetic field,

$$\Delta E(B,T) = \frac{(N_0\alpha - N_0\beta)}{2} x_{\mathrm{Mn}} S B_s\left(\frac{g_{\mathrm{Mn}}\mu_B B}{kT_{\mathrm{eff}}}\right), \qquad (1)$$

where ΔE is the energy shift of the PL line position, B_s is the Brillouin function, N_0 is the number of cation sites in unit volume, α, β are the *s-d*, *p-d* exchange integrals, respectively, taken in our calculations as for the bulk CdMnTe: $N_0\alpha=0.22$ eV and $N_0\beta=-0.88$ eV, $S=5/2$ is the spin of a Mn ion, x_{Mn} is the molar fraction of Mn ions inside the QD; $g_{\mathrm{Mn}}=2$ is the Lande factor for Mn ions, T_{eff} is an effective temperature.

We apply this theory only to the relatively large dots (Fig. 2), because it relies on the assumption of a large extension of the wave function of the carriers and their simultaneous interaction with a large number of magnetic ions. However, in the case of diluted magnetic QDs, the spatial extension of the wave function of the carriers is determined mostly by the zero-dimensional confinement and the number of Mn ions which find themselves inside of the quantum dot is strongly limited. Consequently, the larger the dot the more justified is the use of the MFA and VCA.

From the fits of the experimental data with the Brillouin function we obtain three parameters: the effective temperature $T_{\mathrm{eff}}=4.9$ K, the approximate Mn amount in the QDs $x_{\mathrm{Mn}}=0.0032$ and the position of the PL line at $B=0$ T, 1.7546 eV. The effective temperature is considerably larger than the real temperature of the measurement $T=2$ K, what we attribute to spin-heating effects. Possible contribution of the antiferromagnetic ion-ion interaction to the effective temperature is less likely because of a small concentration of Mn ($x_{\mathrm{Mn}}=0.32\%$) in the dots, although we cannot exclude it completely in view of the fact that even in 6 T the Zeeman shift is not saturated.

We use the effective temperature and the approximate Mn concentration from the Brillouin fit as a starting point for the second step of our calculations: the analysis in terms of the muffin tin model,[16–18] which was commonly used previously for the description of magnetic polarons in the bulk crystals. The basic idea of this model relies on counting all the possible arrangements of Mn ions spins with respect to the direction of the magnetic field. The model assumes also that all Mn spins interact equally strongly with the carriers confined in the QD. However, the exchange energy depends in fact on the position of the Mn ion in the dot. Consequently, in the case of QD containing N_{Mn} ions, we should introduce N_{Mn} additional parameters which describe the position of the each Mn ion in the dot (and at least one parameter describing the size of the QD). Instead of that, the average position of Mn ions inside the dot is introduced in the muffin tin model, and only two fitting parameters are required: average Mn concentration in the dot and the size of the dot.

The question arises, if and when we are justified to average the position of Mn ions inside the QD. It was found by Golnik and Spalek[23] that the calculations in terms of the muffin tin model already with $N_{\mathrm{Mn}}=8$ were consistent with another model[20] of magnetic polarons, where an s-type hydrogenic wave function and continuous changes of the magnetization were assumed. Moreover, the calculations show also a good agreement with the Warnock-Wolff model[24] of magnetic polarons in the case when the ion-ion interaction is absent.[25] This is actually also our case, because of small concentration of Mn ions in the sample.

Summarizing, our model gives reasonable values for the number of Mn ions inside the dot for $N_{\mathrm{Mn}}\geqslant 8$, whereas for smaller N_{Mn} the results can be regarded only as an estimation. The advantage of this approach lies in the possibility of taking the dots sizes into account. The weak point of this model is, as mentioned, that we do not take into account the actual positions of all Mn ions within the QD.

The initial state of the optical transition consists of a system of N_{Mn} Mn ions which interact with an exciton made of a heavy hole and an electron. We assume that the light holes are split off because of the flat cylindrical-like shape of the QDs[26] and can be neglected. Moreover, we assume the simplest, steplike character of the carrier wave function with a constant value inside the QD, while vanishing outside,[16–18] which results in the assumption, that the carriers interact equally strongly with each Mn ion inside the QD and there is no contribution due to ions from outside the dot. Despite this rather crude simplification, we obtain a good agreement with the experimental data (Figs. 2, 3, and 4). It is likely that the good agreement stems from the fact that we count only those Mn that are coupled strongly to the excitons in the quantum dots, whereas the influence of Mn ions lying far from the center of the dot can be neglected. However, the smaller the number of Mn ions inside a QD the more pronounced should be the role of the position of Mn ions inside the QD and, therefore, this model becomes less appropriate.

The energy levels of a diluted magnetic QD with an exciton inside are calculated using the following Hamiltonian:

$$\hat{H}_I = \frac{N_0\alpha x_{\mathrm{Mn}}}{N_{\mathrm{Mn}}}\vec{S}\vec{s} + \frac{N_0\beta x_{\mathrm{Mn}}}{3N_{\mathrm{Mn}}}S_Z j_Z + g\mu_B B S_Z + g_e\mu_B B s_Z + g_{hh}\mu_B B j_Z, \tag{2}$$

where $\vec{S}$ is the operator of the total magnetic moment of N_{Mn} manganese ions,

$$\vec{S} = \sum_{i=1}^{N_{\mathrm{Mn}}} \vec{S}_i$$

and $\vec{s}$ is the spin operator of the electron. S_Z, s_Z, j_Z are the projections of the total Mn magnetic moment, the electron and the hole spin on the direction of the magnetic field with eigenvalues $S_Z=-S,\ldots,S$ $(S=N_{\mathrm{Mn}}\cdot 5/2)$, $s_Z=\pm 1/2$, $j_Z=\pm 3/2$, respectively. The form of the second term in Eq. (2) implies that the hole magnetic moment is locked along the growth axis.

After the recombination of the exciton, the final state of the optical transition consists of a Mn-ion system without any carriers inside and is described by the following Hamiltonian:

$$\hat{H}_F = g\mu_B B_Z \hat{S}_Z. \tag{3}$$

The intensity of the optical transition is calculated from the equation

$$I(E) = \sum_{j_Z,s_Z} \exp\left(-\frac{E_I}{kT}\right) g(S) \left| \left\langle S, S_Z, \frac{3}{2}, j_Z, \frac{1}{2}, s_Z \middle| \hat{\sigma}^{\pm} \middle| S, S_Z \right\rangle \right|^2,$$

$$E = E_I - E_F, \tag{4}$$

where E_I (E_F) is the energy of the initial state (final state) calculated from Eq. (2) [Eq. (3)], $g(S)$ is the degeneracy of the quantum state of N_{Mn} ions with the length of the total spin $\sqrt{S(S+1)}$. The latter quantity is determined by solving a combinatorial problem of counting the number of possible arrangements of the N_{Mn} Mn ions with the magnitude of $S_i=5/2$ leading to total spin S.

We assume that during the recombination of an exciton the arrangement of Mn ions described by the quantum numbers S and S_Z remains unchanged. The operator $\hat{\sigma}^{\pm}$ acting on carrier spins only, does not vanish when $j_Z=3/2$ and $s_Z=-1/2$ or $j_Z=-3/2$ and $s_Z=1/2$. In order to obtain realistic spectra, every line connected with an individual Mn arrangement is broadened by a Lorenz function with the spectral width of 250 μeV taking into account the homogenous broadening of PL lines and spectral resolution in the experiment.

There are three parameters involved in this model. Two of them, the approximate Mn composition x_{Mn} and the effective temperature T_{eff}, have already been crudely determined from the fit of the Brillouin function, $T_{\mathrm{eff}}=4.9$ K and $x_{\mathrm{Mn}}=0.0032$. We use these values as starting points in our fitting procedure. The only new free fitting parameter is the number of Mn ions which reside in the QD. From this parameter we can easily extract the size of the QD using a simple formula, $x_{\mathrm{Mn}}=\frac{N_{\mathrm{Mn}}}{N_{\mathrm{cat}}}$, where N_{cat} is the average number of cation sites the exciton is interacting with in the dot.

With only one new parameter we model the whole magnetic field evolution of the PL lines from individual QDs, including: the redshift of the peak position, narrowing of the spectral width, circular polarization of the lines and the relative intensities of the PL lines at different fields.

Results of the modeling are presented in Figs. 2(b), 3(b), and 4(b), for the large, medium, and small QD, respectively. In the calculations for the large QD, shown in Fig 2(b), we assume exactly the same effective temperature as from the fit with the Brillouin function $T_{\mathrm{eff}}=4.9$ K and a slightly higher molar fraction of Mn $x_{\mathrm{Mn}}=0.0038$ than obtained from the Brillouin fit which describe best the spectral width and the position in the magnetic field. The procedure of finding the number of Mn ions inside the QD, and, therefore, the size of the QD, is presented in Figs. 2(c) and 2(d). In both figures, the solid lines represent results of the calculations of the energy shift and the spectral width for QDs with different sizes but exactly the same $x_{\mathrm{Mn}}=0.0038$ and $T_{\mathrm{eff}}=4.9$ K. The best fit to the experimental data, i.e., to the magnetic field dependence of the energy position and the spectral width, is obtained for a QD containing 25 Mn ions which corresponds to a dot made of 6580 cation sites. The theoretical spectra calculated with these parameters at different magnetic fields are shown in Fig. 2(b).

A slightly different fitting procedure is applied for the calculations presented in Fig. 3(b), for the PL line from the central part of the spectrum. If we assume, that Mn molar fraction in the medium QD is smaller than in the large QD, $x_{\mathrm{Mn}}=0.002$, one can reproduce within the mean field approximation the observed energy shift of 2.7 meV at $B=6$ T. Unfortunately, we are not able to reproduce then the observed spectral widths which are considerably larger than the calculated ones. On the other hand, assuming Mn molar fraction to be nearly the same as in the large QDs, we are in fact able to reproduce both, the spectral position and the spectral width dependence on the magnetic field, which supports a supposition that all the dots are characterized by nearly the same x_{Mn}. To be precise, we begin our fitting procedure in the case of the medium dot with $x_{\mathrm{Mn}}=0.0032$, like in the case of the large QD, while keeping the effective temperature constant, $T_{\mathrm{eff}}=4.9$ K. Then we change x_{Mn} and repeat the fitting. The best fit to the experimental data is obtained, as shown in Figs. 3(c) and 3(d), for QD with $x_{\mathrm{Mn}}=0.0036$ containing 13 Mn ions, which corresponds to a QD consisting of 3600 cation sites. We plotted theoretical evolution of spectra in magnetic field using these parameters in Fig. 3(b).

Exactly the same fitting procedure as for the medium QD, is applied for the small QD [Fig. 4(a)]. We start the fitting again with $x_{\mathrm{Mn}}=0.0032$ and fixed $T_{\mathrm{eff}}=4.9$ K and end up with the Mn content in the dot $x_{\mathrm{Mn}}=0.0034$ and the number of Mn ions inside the dot $N_{\mathrm{Mn}}=5$, which corresponds to a QD consisting of 1450 cation sites.

Please note, that we estimate in fact an average number of cation sites that the exciton confined in the QD is interacting with and not the real number of cations that the QD is made of. At this stage we stress also that we do not include pairs of Mn ions at the nearest neighbors positions in our calculations. However, the probability of finding two Mn ions in the nearest neighbor position is very small in our sample with Mn amount of $x\sim 0.003$. This of course assumes that there is no correlation of Mn incorporation in the QD.

V. CONCLUSIONS

We found a method to introduce only a small number of magnetic ions directly into the CdMnTe QDs. An approximate number of magnetic ions in the QD and the size of the dot itself is found by the analysis of the magnetic field evolution of its PL line, and a comparison of its shape and spectral position to the simulations in terms of the muffin tin model of bound magnetic polaron. In particular, we present results of a large QD containing approximately 25 Mn ions, medium QD with 13 Mn ions inside, and small QD, where the number of Mn ions is estimated to 5. In principle, by further reducing the temperature of Mn effusion cell during the growth of the central CdMnTe layer, we can obtain even smaller number of Mn ions in a repeatable way. The calculated sizes of these QDs indicate that there is a large distribution of the sizes in the ensemble and the number of cation sites the QDs are made of is ranging from 1500 to 6600. Moreover, we found that in order to quantitatively describe effects in the diluted magnetic QDs we must take into account the formation of magnetic polarons.

ACKNOWLEDGMENTS

The authors thank S. Kret for letting us know the preliminary HR TEM studies. This work was supported by the Foundation for Polish Science (Subsidy 8/2003) and SANDIE Network of Excellence.

[1] L. Besombes, Y. Leger, L. Maingault, D. Ferrand, H. Mariette, and J. Cibert, Phys. Rev. Lett. **93**, 207403 (2004).
[2] T. Gurung, S. Maćkowski, L. M. Smith, H. E. Jackson, W. Heiss, J. Kossut, and G. Karczewski, J. Appl. Phys. **96**, 7407 (2004).
[3] S. Mackowski, H. E. Jackson, L. M. Smith, J. Kossut, G. Karczewski, and W. Heiss, Appl. Phys. Lett. **83**, 3575 (2003).
[4] S. Mackowski, J. Wrobel, K. Fronc, J. Kossut, F. Pulizzi, P. C. M. Christianen, J. C. Maan, and G. Karczewski, Phys. Status Solidi B **229**, 469 (2002).
[5] S. Kuroda, N. Itoh, Y. Terai, K. Takita, T. Okuno, M. Nomura, and Y. Masumoto, J. Alloys Compd. **371**, 31 (2004).
[6] S. Kuroda, N. Umakoshi, Y. Terai, and K. Takita, Physica E (Amsterdam) **10**, 353 (2001).
[7] A. V. Scherbakov, A. V. Akimov, D. R. Yakovlev, W. Ossau, L. W. Molenkamp, Y. Terai, S. Kuroda, K. Takita, I. Souma, and Y. Oka, Phys. Status Solidi B **241**, 361 (2004).
[8] G. Bacher, A. A. Maksimov, H. Schomig, V. D. Kulakovskii, M. K. Welsch, A. Forchel, P. S. Dorozhkin, A. V. Chernenko, S. Lee, M. Dobrowolska, and J. K. Furdyna, Phys. Rev. Lett. **89**, 127201 (2002).
[9] G. Bacher, H. Schomig, M. K. Welsch, S. Zaitsev, V. D. Kulakovskii, A. Forchel, S. Lee, M. Dobrowolska, J. K. Furdyna, B. Konig, and W. Ossau, Appl. Phys. Lett. **79**, 524 (2001).
[10] J. Seufert, G. Bacher, M. Scheibner, A. Forchel, S. Lee, M. Dobrowolska, and J. K. Furdyna, Phys. Rev. Lett. **88**, 027402 (2002).
[11] S. Lee, M. Dobrowolska, and J. K. Furdyna, Phys. Rev. B **72**, 075320 (2005).
[12] A. A. Maksimov, G. Bacher, A. McDonald, V. D. Kulakovskii, A. Forchel, C. R. Becker, G. Landwehr, and L. Molenkamp, Phys. Rev. B **62**, R7767 (2000).
[13] A. Hundt, J. Puls, and F. Henneberger, Phys. Rev. B **69**, 121309(R) (2004).
[14] P. R. Kratzert, J. Puls, M. Rabe, and F. Henneberger, Appl. Phys. Lett. **79**, 2814 (2001).
[15] F. Tinjod, I. C. Robin, R. Andre, K. Kheng, and H. Mariette, J. Alloys Compd. **371**, 63 (2004).
[16] A. Golnik, J. Ginter, and J. A. Gaj, J. Phys. C **16**, 6073 (1983).
[17] S. M. Ryabchenko and Yu. G. Semenov, Sov. Phys. JETP **57**, 825 (1983).
[18] T. H. Nhung, R. Planel, C. Benoitala Guillaume, and A. K. Bhattacharjee, Phys. Rev. B **31**, 2388 (1985).
[19] F. Tinjod, B. Gilles, S. Moehl, K. Kheng, and H. Mariette, Appl. Phys. Lett. **82**, 4340 (2003).
[20] T. Dietl and J. Spalek, Phys. Rev. B **28**, 1548 (1983).
[21] S. Maćkowski, Thin Solid Films **412**, 96 (2002).
[22] K. Sebald, P. Michler, T. Passow, D. Hommel, G. Bacher, and A. Forchel, Appl. Phys. Lett. **81**, 2920 (2002).
[23] A. Golnik and J. Spalek, J. Magn. Magn. Mater. **54-57**, 1207 (1986).
[24] J. Warnock and P. A. Wolff, Phys. Rev. B **31**, 6579 (1985).
[25] A. Golnik and J. Spalek (unpublished).
[26] F. V. Kyrychenko and J. Kossut, Phys. Rev. B **70**, 205317 (2004).